Mechanism of Enolase: The Crystal Structure of Enolase–Mg^{2+}–2-Phosphoglycerate/Phosphoenolpyruvate Complex at 2.2-Å Resolution[†,‡]

Lukasz Lebioda* and Boguslaw Stec[§]
Department of Chemistry, University of South Carolina, Columbia, South Carolina 29208
Received June 6, 1990; Revised Manuscript Received November 19, 1990

ABSTRACT: Enolase in the presence of Mg^{2+} catalyzes the elimination of H_2O from 2-phosphoglyceric acid (PGA) to form phosphoenolpyruvate (PEP) and the reverse reaction, the hydration of PEP to PGA. The structure of the ternary complex yeast enolase–Mg^{2+}–PGA/PEP has been determined by X-ray diffraction and refined by crystallographic restrained least-squares to an $R = 16.9\%$ for those data with $I/\sigma(I) \geq 2$ to 2.2-Å resolution with a good geometry of the model. The structure indicates the substrate molecule in the active site has its hydroxyl group coordinated to the Mg^{2+} ion. The carboxylic group interacts with the side chains of His373 and Lys396. The phosphate group is H-bonded to the guanidinium group of Arg374. A water molecule H-bonded to the carboxylic groups of Glu168 and Glu211 is located at a 2.6-Å distance from carbon-2 of the substrate in the direction of its proton. We propose that this cluster functions as the base abstracting the proton in the catalytic process. The proton is probably transferred, first to the water molecule, then to Glu168, and further to the substrate hydroxyl to form a water molecule. Some analogy is apparent between the initial stages of the enolase reverse reaction, the hydration of PEP, and the proteolytic mechanism of the metallohydrolases carboxypeptidase A and thermolysin. The substrate/product binding is accompanied by large movements of loops Ser36–His43 and Ser158–Gly162. The role of these conformational changes is not clear at this time.

Enolase (EC 4.2.1.11) is a glycolytic enzyme which catalyzes the dehydration of 2-phospho-D-glycerate to phosphoenolpyruvate (eq 1). The reaction involves only a small free

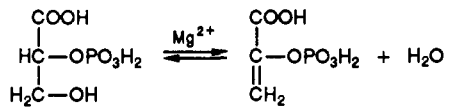

(1)

energy change of about 1 kcal/mol, and the reverse reaction is utilized in gluconeogenesis (Wold, 1971). The enolase reaction is intriguing from a mechanistic point of view, since it involves the abstraction of a relatively nonacidic proton and the elimination of an OH^- which is a poor leaving group. The mechanism of action has been investigated, and it was concluded (Dinovo & Boyer, 1971; Stubbe & Abeles, 1980) that the dehydration reaction is a two-step process involving, initially, the abstraction of the hydrogen from C(2) as a proton to form a carbanion and then the elimination of the OH^- group and the formation of a double bond between C(2) and C(3).

All known enolases exhibit an absolute requirement for certain divalent cations for enzymatic activity, of which the natural cofactor Mg^{2+} gives the highest activity (Brewer, 1981). As isolated, the yeast enzyme contains endogenous tightly bound Mg^{2+}. The enzyme may be stripped of its endogenous Mg^{2+} and almost any other ion substituted. The enzyme binds 1 mol per subunit of Mg^{2+}, Sm^{3+}, Tb^{3+}, Co^{2+}, Ni^{2+}, Zn^{2+}, and probably most other divalent metal ions (Brewer et al., 1983). Metal ion binding at this site is called "conformational". Not all conformational metal ions activate the enzyme, but there is no specificity for those which produce activity. Indeed, Ca^{2+}, Tb^{3+}, and Sm^{3+} which do not activate enolase bind tighter than Mg^{2+}.

A conformational metal ion must be present for substrate/product or substrate–analogue binding (Hanlon & Westhead, 1969; Faller et al., 1977). No catalysis occurs upon substrate binding. However, in the presence of substrate, additional metal ion binding can take place. This additional metal binding produces catalysis; thus, the second metal ion is termed "catalytic".

It was proposed that the hydroxyl on C(3) of the substrate 2-phospho-D-glycerate coordinates directly to the conformational metal ion (Mildvan, 1970), and subsequent evidence (Nowak et al., 1973; Anderson et al., 1984) corroborated this hypothesis. Several hypotheses were put forward which assigned the role of the catalytic base to different moieties. Nowak et al. (1973) proposed the phosphate group of the substrate. Brewer (1985) suggested a water molecule coordinated to the conformational metal ion. Weiss et al. (1987) proposed the single sulfhydryl, Cys273, in yeast enolase as the base required for removal of the proton (or deuterium) from C(2) of the substrate. These proposals were made, however, without the knowledge of 3-D structure.

Recently, the crystal structure of yeast apoenolase was determined (Lebioda et al., 1989) and refined at 2.25-Å resolution (Stec & Lebioda, 1990). The molecule is a dimer of identical subunits related by a crystallographic 2-fold axis of symmetry. Each subunit is built of two domains. The smaller N-terminal domain is based on a three-stranded antiparallel β-meander and four α-helices. The main domain is an 8-fold $\alpha+\beta$-barrel similar to that of the triosephosphate isomerase (TIM) barrel. However, the enolase barrel has a $\beta\beta\alpha\alpha(\beta\alpha)_6$ topology which is different from the $(\beta\alpha)_8$ topology of the TIM barrel. Consequently, the second β-strand in the enolase barrel is antiparallel to the other β-strands, and the first α-helix is antiparallel to other α-helices.

[†] This work was supported by the National Institutes of Health (Grant GM34994).

[‡] The atomic coordinates for the structure of enolase–Mg^{2+}–2-phosphoglycerate/phosphoenolpyruvate have been deposited to the Brookhaven Protein Data Bank as entry 7ENL.

[§] Permanent address: SLAFIBS, Jagiellonian University, Cracow, Poland.

0006-2960/91/0430-2817$02.50/0

Table I: Summary of Parameters and Results of Restrained Refinement

	σ	final rms
distances (Å)		
bond length (1–2 neighbors)	0.020	0.015
bond angles (1–3 neighbors)	0.040	0.051
planes (1–4 neighbors)	0.050	0.071
planar groups (Å)	0.020	0.012
chiral vol (Å^3)	0.150	0.175
nonbonded contacts (Å)		
single-torsion contacts	0.45	0.23
multiple-torsion contacts	0.45	0.28
possible H-bonding contacts	0.45	0.33
torsion angles (deg)		
peptide plane (ω)	3.0	3.4
staggered (±60°, 180°)	12.0	20.2
orthonormal (±90°)	16.0	30.9
wt for diffraction data	$s = 7.0 - 42.0 (\sin\theta/\lambda - {}^1/_6)$	
	$s = 0.0$ for $I < 2\sigma(I)$	
final R for all reflections		0.201
Luzzati estimate of coordinates error (Å)		0.25

The structure of holoenolase in the form of the enolase–Zn^{2+} complex was refined by the restrained least-squares method to an R = 14.9% at 1.9-Å resolution (Lebioda & Stec, 1989). The ligands of Zn^{2+} in the conformational site form an almost regular trigonal bipyramid with two monodentate carboxylic groups of Asp246 and Asp320 in the axial positions while two water molecules and monodentate Glu295 are in the equatorial positions. So far, it was generally assumed that the coordination of the conformational metal ion in enolase was octahedral. This, however, was based on the Mg^{2+} propensity for octahedral coordination rather than data. In the enolase–Mn^{2+} complex, Nowak et al. (1973) found two rapidly exchanging water and two or three carboxylic ligands. This is in excellent agreement with our crystallographic data.

It should be emphasized that the enzyme is active at the conditions (pH 5, 50% saturated ammonium sulfate) fairly close to those in the crystals although the K_m values for Mg^{2+} and the substrate are much larger and the V_{max} is only 5% of the value obtained under standard assay conditions (Lebioda et al., 1989). We report here additional X-ray structural studies performed on crystals of yeast enolase and some speculations, based on these results, about the mechanism of enolase catalysis.

Materials and Methods

Crystals of yeast enolase suitable for X-ray diffraction studies were grown by the vapor diffusion methods as described previously (Lebioda & Brewer, 1984). A solution containing equal volumes of 3% enolase, 2 mM Mg^{2+}, 1 mM EDTA, 1 mM dithiothreitol, 0.05 M citrate buffer (pH 5.0), and 55% saturated ammonium sulfate was equilibrated against 55% saturated ammonium sulfate solution. The crystals were transferred to a solution of 75% saturated ammonium sulfate, 0.025 M citrate buffer, pH 6.0, and 20 mM Mg^{2+}, which was gradually made 20 mM in PGA. The crystals were quite resistant to the pH and ammonium sulfate and Mg^{2+} concentration changes but were affected by PGA. This sensitivity is due to the changes in the unit dimensions. Native crystals at pH 5 and enolase–Zn^{2+} crystals at pH 6 have the same unit cell dimensions within experimental error: $a = b = 124.1$ Å, $c = 66.9$ Å. The crystals of the precatalytic ternary complex enolase–Mg^{2+}–PGA/PEP have $a = b = 122.0$ Å, $c = 67.0$ Å. Thus, the a and b lattice parameters shrunk 1.7% in the presence of substrate. Some crystals nonetheless survived the soaking process without cracking. The data were collected with a Xentronic area detector and processed by using XENGEN software. A total of 38 215 observations in the 8–2.2-Å resolution were merged and yielded 21 660 symmetry-independent reflections with R_{int} = 7.5%; 16 196 reflections with $I > 2\sigma(I)$ were used in the structure refinement.

The structure of the binary complex enolase–Zn^{2+} (Lebioda & Stec, 1989) was used as the starting model. The positions of the side chains in the environment of the substrate were refitted to omit difference Fourier maps. The dictionary for the PGA molecule was constructed by using the bond lengths and bond angles found in the crystal structure of trisodium 2-phospho-D-glycerate hexahydrate (Lis, 1985). The restraints were the same as for the protein model except that no restraints on the torsion angles of the substrate molecule were applied. The molecule of PGA was positioned in the electron density maps calculated by using phases computed from the refined protein prior to the inclusion of the ligand in the refinement. We did not attempt to model PGA/PEP disorder because the overlap of their positions is very tight. The structure refinement by restrained least squares was carried out by using the PROLSQ program (Hendrickson & Konnert, 1980). The final values of the refinement parameters are given in Table I and the distribution of R factors in Table II.

Results and Discussion

Structure. The refined structure is very similar to the structures of apoenolase (Stec & Lebioda, 1990) and the enolase–Zn^{2+} complex (Lebioda & Stec, 1989). For the most part, the differences in the atomic positions are not significant, with the exception of two loops discussed below. The average temperature factors calculated for each residue are very similar to those for apoenolase (Stec & Lebioda, 1990). The ordered solvent is also very similar to the one found previously except for the active site, where two water molecules were displaced by the substrate molecule, and the loops region. Altogether, 346 water molecules, which represent about 15% of the total solvent in the unit cell, were included in the refined model.

Active-Site Geometry. The active site is located in a deep cavity at the carboxylic end of the β-barrel (Figure 1). Similar locations of the active sites were found in all other enzymes with an 8-fold β/α-barrel structure. The active-site residues are on all β-strands of the barrel with the exception of the first strand.

The electron density found as a result of the substrate/product binding is shown in Figure 2. The electron density at the phosphate position is very high, 11σ, and approximately spherical as expected. The highest density in the organic part of the substrate molecule is about 7σ. While the location of the phosphate moiety is, in our judgment, unquestionable, the positioning of the organic part is somewhat less obvious though also sound. Its electron density forms a relatively flat lobe connected to the phosphate density. The carboxylic group and the hydroxyl cannot be distinguished. With the phosphate moiety held in its density, the substrate can be positioned either with the hydroxyl coordinated to the metal ion as shown in Figure 2 or with the carboxylic group coordinated to the metal ion in a monodentate fashion. In this last case, however, the noncoordinating oxygen atom of the carboxylate is clearly

Table II: Number of Reflections with $I > 2\sigma(I)$ and R Factors as a Function of Resolution

D_{min} (Å)	4.5	3.5	3.0	2.8	2.6	2.4	rest	total
no. of reflections	2050	2804	2809	1537	1858	2115	2023	16.196
R (%)	18.5	14.0	16.1	17.8	18.7	19.0	18.7	16.9

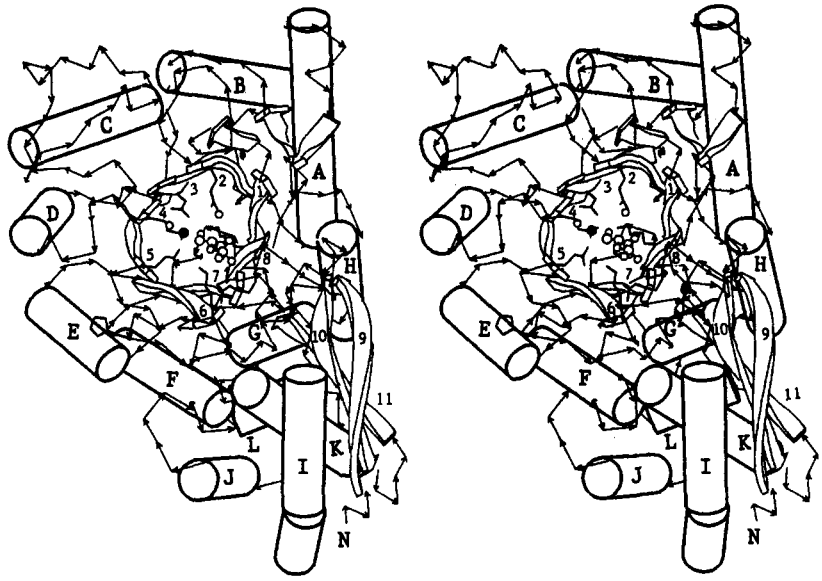

FIGURE 1: Stereoview of the subunit of enolase seen approximately along the barrel axis. The active site is located in the deep cavity at the carboxylic end of the barrel. The position of the conformational metal ion is marked with a filled circle. The PGA molecule and two water molecules in the active site are drawn with open circles. The main secondary structure elements are denoted according to the previous notation (Lebioda et al., 1989). The sequence of secondary structure elements along the peptide chain is N-9, 10, 11, I, J, K, L, 1, 2, A, B, 3, C, D, 5, E, 6, F, 7, G, 8, H–COOH. The side chains of the active-site residues are drawn as stick models. From β-strand: 2 branches, Glu162; 3, Asp246; 4, Glu295; 5, Asp320; 6, Lys345; 7, Arg-374; and 8, Lys396.

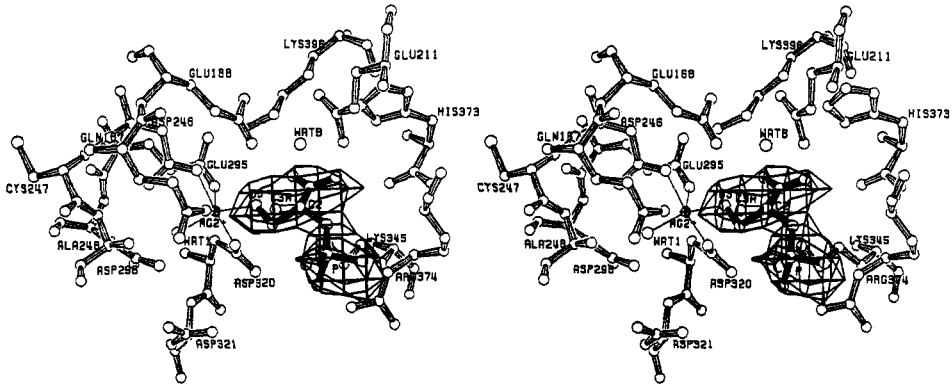

FIGURE 2: Active site of enolase. The electron density, contoured at the 2.5σ level, is from a difference Fourier map phased with a model in which the substrate molecule was omitted. The PGA molecule is drawn with heavy lines. The water molecule postulated as the catalytic base is denoted as WATB. For the product, PEP, the modeled position of carbon-3 is denoted C3A, and the C(2)–C(3A) bond is drawn without shading. The modeled position of the product water molecule is somewhat below O(3) (not shown because of overlap). The temperature factors for the active-side residues refined in the 10–20 Å^2 range, and for the substrate, 38–41 Å^2.

sticking out of the electron density. There is no explanation for part of the density between the carboxylate and the hydroxyl, and in general the fit of the model to the density is worse. The initial map phased by the model derived from the binary complex was very similar to the one shown in Figure 2 except that the density connecting the two lobes, phosphate and organic, was weaker.

Although we do not see in the electron density the "catalytic" Mg^{2+} ion, as discussed below, it must be bound to a small fraction of molecules constituting the crystal because the enzyme is active at the conditions similar to these in the crystals. The time during which the crystal was mounted and aligned on the diffractometer was most likely sufficient to approach the reaction equilibrium because the volume of mother liquor was very small and the concentration of enolase in the crystal very high, about 10 mM. We estimated that the ratio of substrate to enzyme molecules was less than 10.

The electron density in the area of C(3) and the hydroxyl is fairly bloated and indicates some averaging of the substrate, PGA, and the products, PEP and H_2O molecules. The two species should be bound in the active site with about a 1:1 ratio (Faller et al., 1977; Brewer & Ellis, 1983). The elimination of the water molecule from PGA is specifically anti; i.e., the hydroxide ion and proton leave from the opposite sides of the carbon atom plane (Cohn et al., 1969) so very approximate positions of the products can be figured out.

The electron density itself, although indicating disorder, does not offer a clue as to how to build the model for the alternate positions of C(3) and O(3). On the other hand, the electron density for the carboxylic group is quite well-defined and even on very low contouring levels does not indicate disorder. It appears that the PGA molecule is bound in a conformation different from that found in the crystals of the potassium salt of PGA. There, the plane of the carboxylic group is perpendicular to the plane of the three carbon atoms (Lis, 1985) while in the complex with enolase the electron density indicates a conformation with the carboxylic group and the C(2) and C(3) atoms approximately in one plane. Some distortion of substrate analogues bound to enolase in the presence of activating metal ions was observed before using absorption spectroscopy (Brewer & Collins, 1980). Interestingly, nonactivating metal ions (e.g., Ca^{2+}) do not induce the distortion (Brewer, un-

published results). The coplanar conformation also was found in the crystal structures of several salts of PEP (Lis, 1987). It should be indicated here that the phosphate part of the substrate and product molecules appears to be flexible. In the small-molecule crystals, several different conformations of the phosphate moiety also were observed as a result of different crystal packing.

The structure of the ternary complex confirms the trigonal bipyramidal coordination of the metal ion which was found in the binary enolase–Zn^{2+} complex (Lebioda & Stec, 1989). The relatively wobbly 5-fold coordination probably facilitates ligand exchange at the metal ion and prevents the formation of too stable enzyme–substrate complexes. Of the two water molecules coordinated to the Zn^{2+} in the binary complex, the one with a high temperature factor reacts with the PEP molecule or is replaced by the hydroxyl group of the PGA molecule.

The carboxylic group of the substrate is 3.0 Å from one of the δ-atoms of His373. At resolutions achievable with protein crystals, X-ray diffraction experiments do not allow one to distinguish between C and N atoms; the orientation of imidazole and amide moieties is usually guessed from the environment suitable for the formation of hydrogen bonds. In the structures of apoenolase and the enolase–Zn^{2+} complex, we have positioned the imidazole ring of His373 so that it forms a hydrogen bond to the water molecule WATB; the $N_{\epsilon 2}$–O distance refined to 3.0 Å. In the ternary complex, this distance is 3.3 Å while the distance between O(2) of the substrate and $C_{\delta 2}$ of His373 is 3.0 Å. The precision of the structure is insufficient to decide, based on the distances, which of the contacts is indeed the H bond; the directions of the N–H bonds are favorable in both orientations. The interaction with the carboxylate should be, however, more favorable because of the charges involved. We therefore think that it is likely that the side chain of His373 is flipped 180° and forms a hydrogen bond through its $N_{\delta 1}$ atom to the substrate molecule rather than to the water molecule. The other oxygen atom of the substrate carboxylate, O(1), is 3.2 Å from the N_{ξ} atom of Lys396.

The phosphate group forms an ion pair with Arg374 and occupies the sulfate binding site found in the apoprotein (Lebioda et al., 1989) and in the binary complex. The position of the phosphate is about 1.0 Å from the position of the sulfate, toward the conformational cation binding site. The side chain of Arg374 is in an all g^- conformation as it is in apoenolase and in the binary complex. It appears, however, that the phosphate group is not in contact with the side chain of Ser375 as is the sulfate ion. The distance between the closest O atom of the phosphate group and O_{γ} of Ser375 is 4.4 Å while for the sulfate ion the corresponding distance is 3.1 Å. Also, out of the two contacts between the $N_{\eta 2}$ and N_{ϵ} atoms, and the sulfate oxygens 2.6 and 2.8 Å, respectively, with good H-bond geometry, only the first one is obvious in the ternary complex. The corresponding distances are 3.1 and 3.6 Å. It may be speculated that this less tight interaction creates the binding site for the catalytic metal ion at the phosphate moiety.

The C(2) atom of the substrate molecule is close to a water molecule denoted WATB on Figure 2; the distance is 2.6 Å. In the binary complex, this water molecule has an approximately tetrahedral coordination with the carboxylic groups of Glu168 and Glu211 contributing one O_{ϵ} atom each, presumably serving as H-bond acceptors, while $N_{\epsilon 2}$ of His373 and another water molecule, O515, are H-bond donors. In the ternary complex, the water molecule O515 is displaced by the C(2) atom of the substrate while WATB is shifted 0.35 Å

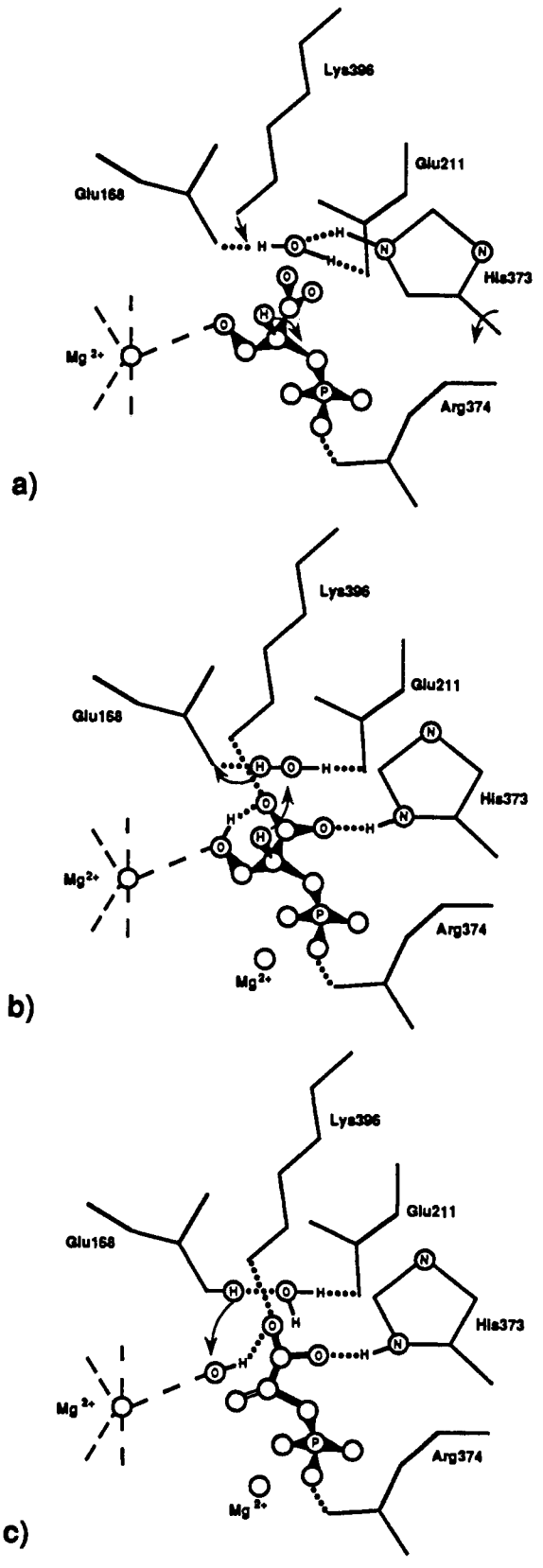

FIGURE 3: Proposed mechanism of dehydration of PGA to PEP by enolase. The arrows represent the movements of atoms in (a) conformational changes in (b and c) proton transfers.

away from the imidazole. The imidazole group of His373 is probably flipped and positioned with the $C_{\epsilon 1}$ atom toward the WATB molecule while H-bonded to the substrate carboxyl as discussed above. In this environment, rich in negative charges, the imidazole is almost certainly protonated. We want to emphasize that the proposed imidazole flip is based on the

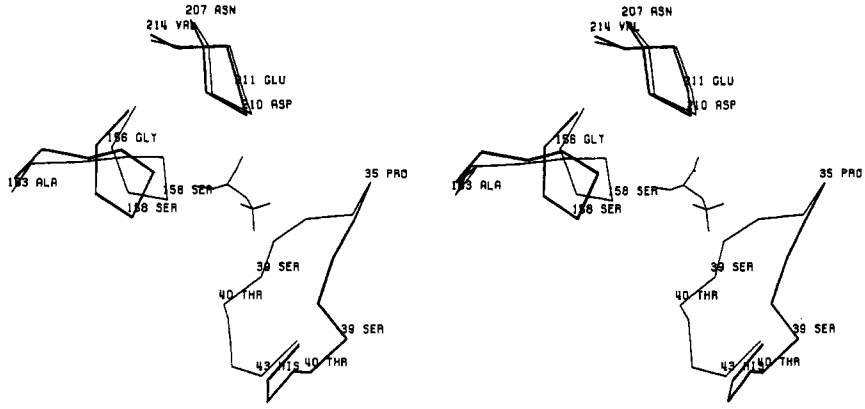

FIGURE 4: Stereoview of the C_α plot of the moveable loops. Heavier lines correspond to the main chain in the binary complex enolase–Zn^{2+}, lighter to the precatalytic ternary complex. The position of the substrate is also shown (center).

above analysis of the electrostatic charges in its environment, not on X-ray diffraction evidence.

Accuracy of the Data. An analysis of the data using Luzzati plots (Luzzatti, 1952) gave 0.25 Å as an estimate of the accuracy of atomic positions.

Mechanism of Enolase. The structure of the enzyme–substrate complex is a good starting point for speculations about the enzyme mechanism. The water molecule, WATB, H-bonded to two carboxylic groups (Figure 2) should be strongly polarized and nucleophilic. We propose that this water molecule, which is next to C(2), acts as the base abstracting the proton in the dehydration reaction. This hypothesis is based on the position of the water molecule and on the measurements of the equilibrium isotope effect in the inhibition of enolase by tartronate semialdehyde phosphate (an aldehyde analogue of PGA with the hydroxyl group replaced by the aldehyde oxygen). The inhibition data indicated a fractionation factor of hydrogen/deuterium on the catalytic base of about 0.4 for both yeast and rabbit muscle enolase (Weiss et al., 1987). Out of all protein functional groups, only the sulfhydryl group has a fractionation factor significantly below 1.0, and that is 0.43 (Cleland, 1980). However, there is no cysteine in the active site of enolase. Also, the single cysteine in the yeast sequence is not conserved in the homologous muscle enzyme. The two enzymes have a 60% sequence identity, and their structures should be very similar, especially in the active-site region. There are multiple determinations of the sequences and errors there are not probable. Thus, cysteine is a highly unlikely candidate for the catalytic base for any of these two reasons.

The H_3O^+ species also have an H/D fractionation index that is significantly below 1.0. Cleland (1980) lists 0.69, but the exact value could be dependent on the environment of a hydronium ion because the isotope effect is influenced by its hydrogen-bond properties in a manner dependent on the H-bond length (Olovsson & Jönson, 1976). Thus, the mechanistic studies (Weiss et al., 1987) could be interpreted as indicating the water molecule as the catalytic base.

The neighborhood of the two glutamates must be essential for the water molecule basicity, and the cluster should be in the tautomeric equilibrium.

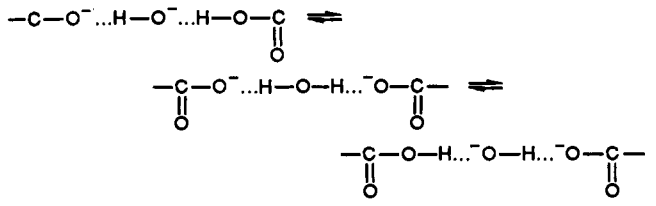

A direct transfer of the proton to Glu168 is certainly a possibility (see Figure 2), but the H/D fractionation factor for the carboxylic group is 1.00 (Cleland, 1980). We would like to emphasize that although crystallography suggested and supports the "go between" role of the water molecule (between the substrate molecule and Glu168), direct transfer of the proton certainly is an alternative. The decisive evidence lies in the measurements carried out by the Cleland group (Weiss et al., 1987).

The rate of the enolase reaction is controlled by the catalytic metal ion (Brewer, 1981). We have not positively identified any feature in the electron density maps that could be interpreted as the second, catalytic Mg^{2+} ion. We think that the high ionic strength of the mother liquor increases its dissociation constant to the extent that the electron density of the bound catalytic metal ion is not above the noise level of the map. The most probable location of the catalytic metal ion binding site is at the phosphate group (Brewer & Ellis, 1983). At a 1.3σ contouring level, we see some electron density extending toward solvent from the O(2P) oxygen atom of the phosphate group. O(2P) is the most distant atom from Arg374, but the significance of this electron density is uncertain. The stressed and weakened interaction of the phosphate group with Arg374, when compared to the sulfate binding, suggests an increased affinity of the phosphate group for another ligand. The additional positive charge at the phosphate group should lead to electron withdrawal from C(2) and in consequence facilitate the proton removal (Borders et al., 1978).

The electron density in the Fourier maps for Lys396 is strong, but cylindrical, and the actual position of N_ξ is not obvious. In the extended conformation, the N_ξ–O(1) distance of 3.2 Å is appropriate for H-bond formation, but the N_ξ charge is partially neutralized by the carboxylate of Glu295 which is also at a H-bonding distance. It is also possible that the conformation of the side chain of Lys396 changes in the transition state, resulting in a weaker interaction with Glu295 and further stabilization of the negative charge at the substrate carboxyl. This would lead to further decrease of electron density at C(2).

It appears likely that the proton abstracted from C(2) is transferred further to Glu168, which has a relatively hydrophobic environment, and later to the hydroxyl group of the PGA molecule.

The terminal part of the enolase reaction seems to mirror the relatively well-understood mechanism of carboxypeptidase A and thermolysin (Christianson & Lipscomb, 1989; Matthews, 1988). The mechanism of these enzymes is usually

analyzed as the hydrolysis of the peptide bond, so comparison is easier if these are compared with the hydration of PEP. In each of the three enzymes, there is a water molecule activated by coordination to a small divalent metal ion, Zn^{2+} in proteases and Mg^{2+} (or Zn^{2+}) in enolase. The position of this water molecule, which should not be confused with WATB, approximately corresponds to the position of the O3 atom of the substrate (Figure 2). The water molecule activation is assisted by a neighboring glutamic acid residue, Glu270 in carboxypeptidase A, Glu143 in thermolysin, and Glu168 in enolase, and leads to a nucleophilic, hydroxide-like species. The hydroxide attacks the trigonal carbon atom, forming a tetrahedral intermediate. Such interpretation is supported by the geometry of the complexes. In the binary complex enolase–Zn^{2+}, where there is no disorder and the coordinates are relatively very well determined, the distance between the metal-coordinated H_2O molecule and O_ϵ of Glu168 is 2.7 Å, indicating a strong interaction. Studies of the complex of enolase with PEP and a nonactivating metal ion should provide some more details of this phase of catalysis.

The proposed mechanism for enolase-catalyzed dehydration of PGA as the forward reaction is summarized in Figure 3.

Loop Movement. The conformation of the enzyme molecule is essentially the same in the binary enolase–Zn^{2+} complex and the precatalytic ternary complex. The exceptions to this are two loops which show considerable movement (Figure 4). Loop Pro35–His43 from the first domain is flexible in the binary complex as can be judged from the relatively high temperature factors of those residues. In the ternary complex, this loop moves toward the active site, apparently closing on the substrate molecule. The electron density of the loop is poor, and there are no large side chains in the loop. Thus, the conformation of the loop is only tentative. Another loop, Gly156–Ala163, also shows some displacement, though smaller. The movements of these loops appear to close the active-site cavity off from the solvent somewhat. Otherwise, the significance of their movement is not clear at this point.

Conclusions

The crystal structure of the precatalytic ternary complex of enolase is a good starting model for speculations about the enzyme mechanism. The active site of enolase is quite rigid, and we did not see large conformational changes upon substrate binding there. At earlier stages of enolase studies, we used the single sulfate binding site to model the mode of substrate binding. The molecule of PGA was docked with the phosphate group in the sulfate site and the hydroxyl at the conformational Mg^{2+} site. It is encouraging to note that these modeling studies were, in retrospect, very successful and led to speculations similar to those obtained with the actual substrate binding data. On the other hand, two loose loops relatively distant from the active site move into the vicinity of the substrate; their movement obviously could not be guessed.

The active site is complementary to a conformational and electronic state of the substrate that is closer to the product and probably the transition state. The structure suggested the reinterpretation of the mechanistic data, which are now consistent with the dogma of conservation of active-site residues during evolution.

The knowledge of the structure of the precatalytic complex makes it possible to rationally design mutants of enolase which could probe the enzyme mechanism. Further crystallographic experiments are needed, however, to find the catalytic metal ion binding site, to elucidate the reasons for the lack of enzyme activation by Ca^{2+} ions, and to examine other aspects of enolase function. The ability to control enolase activity through control of metal ion concentration and selection of activating or nonactivating metal ions offers an almost unique opportunity that should allow delineation of various stages along the reaction pathway and make it a significant study of metalloenzyme mechanisms.

Acknowledgments

We thank M. Deacon and E. M. Westbrook for help with the data collection at the Midwest Area Diffractometer Facility and J. M. Brewer for the gift of purified enolase and stimulating discussions.

References

Anderson, V. E., Weiss, P. M., & Cleland, W. W. (1984) *Biochemistry 23*, 2279–2286.
Borders, C. L., Woodall, M. L., & George, A. L. (1978) *Biochem. Biophys. Res. Commun. 82*, 901–904.
Brewer, J. M. (1981) *CRC Crit. Rev. Biochem. 11*, 209–254.
Brewer, J. M. (1985) *FEBS Lett. 182*, 8–14.
Brewer, J. M., & Collins, K. M. (1980) *J. Inorg. Biochem. 13*, 151–164.
Brewer, J. M., & Ellis, P. D. (1983) *J. Inorg. Biochem. 18*, 71–81.
Brewer, J. M., Carreira, L. A., Collins, K. M., Duvall, M. C., Cohen, C., & Dervartanian, D. V. (1983) *J. Inorg. Biochem. 19*, 255–267.
Christianson, D. W., & Lipscomb, W. N. (1989) *Acc. Chem. Res. 22*, 62–69.
Cleland, W. W. (1980) *Methods Enzymol. 64*, 108–125.
Cohn, M., Pearson, J. E., O'Connell, E. L., & Rose, I. A. (1970) *J. Am. Chem. Soc. 92*, 4095–4098.
Dinovo, E. C., & Boyer, P. D. (1971) *J. Biol. Chem. 246*, 4586–4593.
Faller, L. D., Baroudy, B. M., Johnson, A. M., & Ewall, R. X. (1977) *Biochemistry 16*, 3864–4869.
Hanlon, D. P., & Westhead, E. W. (1969) *Biochemistry 8*, 4247–4254.
Hendrickson, W. A., & Konnert, J. H. (1980) in *Biomolecular Structure, Function, Conformation, and Evolution* (Srinivasan, R., Ed.) pp 43–57, Pergamon Press, Oxford.
Lebioda, L., & Brewer, J. M. (1984) *J. Mol. Biol. 180*, 213–215.
Lebioda, L., & Stec, B. (1989) *J. Am. Chem. Soc. 111*, 8511–8513.
Lebioda, L., Stec, B., & Brewer, J. M. (1989) *J. Biol. Chem. 264*, 3685–3693.
Lis, T. (1985) *Acta Crystallogr. C41*, 1578–1580.
Lis, T. (1987) *Acta Crystallogr. C43*, 1898–1900.
Luzzati, V. (1952) *Acta Crystallogr. 5*, 802–810.
Matthews, B. W. (1988) *Acc. Chem. Res. 21*, 333–340.
Mildvan, A. S. (1970) *Enzymes (3rd Ed.) 3*, 445.
Nowak, T., Mildvan, A. S., & Kenyon, G. L. (1973) *Biochemistry 12*, 1690–1701.
Olovsson, I., & Jönson, P.-G. (1976) in *The Hydrogen Bond—Recent Developments in Theory and Experiments* (Schuster, P., et al., Eds.) pp 394–456, North-Holland Publishing Co., Amsterdam.
Stec, B., & Lebioda, L. (1990) *J. Mol. Biol. 211*, 235–248.
Stubbe, J.-A., & Abeles, R. H. (1980) *Biochemistry 19*, 5505–5512.
Weiss, P. M., Boerner, R. J., & Cleland, W. W. (1987) *J. Am. Chem. Soc. 109*, 7201–7202.
Wold, F. (1971) *Enzymes (3rd Ed.) 5*, 499–508.